

Fig. 4. Energy density spectra of the quiet ring current at constant L : (a) 6-7, (b) 5-6, (c) 4-5, and (d) 3-4. Error bars are an average of the uncertainty associated with single orbit passes. H^+ (solid circle), O^+ (open circle), He^+ (solid square), and He^{++} (solid triangle).

Asymmetrical ring currents have been predicted for quiet times [Alfvén, 1939; Wolf, 1974], as well as having been observed during storms [Fukushima and Kamide, 1973; Roelof, 1987]. We plot in Figure 5 proton energy density profiles in four quadrants centered on midnight, dawn, noon, and dusk. The x axis is L^* , an L shell value corrected for a distorted dipole and is therefore largely free from magnetic L shell splitting effects. There still remains a noon-midnight asymmetry for $L > 5$, giving way to a dawn-dusk asymmetry for $L > 3$ with a maximum amplitude of about 40% in both regions. Below $L \sim 3$, the asymmetry is less than the variance in the orbits. The dawn-dusk asymmetry agrees with the more si-

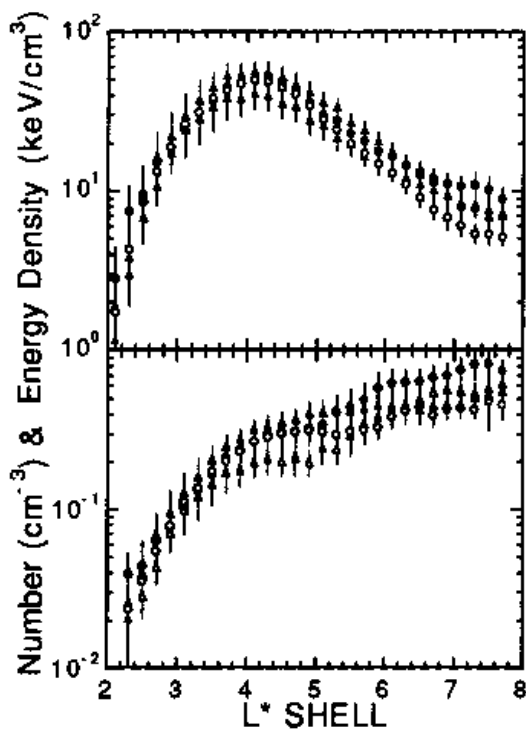


Fig. 5. Proton energy and number density profiles of the quiet ring current in four quadrants centered on midnight (solid circle), dawn (open triangle), noon (open circle), and dusk (solid triangle), where magnetic shell splitting effects have been largely removed.

multaneous Viking data [Stüdemann *et al.*, 1987] as well as the contours of Sugiura [1972]. For $L > 6$, the densities are higher in the midnight sector, consistent with its proximity to the presumed source region in the magnetotail. Below $L \sim 5$, however, the dusk sector dominates, which we attribute to electric field L shell splitting. That is, because convection electric fields slightly distort $E > 100$ keV circular drift paths, dusk becomes the "perigee" sector for these drift orbits, and the stronger magnetic field at perigee implies higher ionic densities and energies [Wolf, 1983].

Data Set Preparation

Since the standard radial diffusion solutions are naturally expressed as phase space densities in magnetic moment and L shell (M - L space), we have smoothed and interpolated the data bins in this coordinate system. We collected dJ/dE in 32 energy/charge bins, 33 L^* bins, 4 LT bins and 3 yearly temporal bins. We first averaged the background-subtracted fluxes over all LT and temporal bins, zeroing the negative fluxes caused by overestimating the background. We smoothed the logarithms of the averaged fluxes using a uniform β spline interpolation [Bartels *et al.*, 1983], we also constructed the interpolating piecewise continuous polynomials for the next step. We then interpolated from energy to magnetic moment grid using the local magnetic field magnitude, using 3-cycle averages from the magnetometer (CCB magnetometer kindly supplied by L. Zanetti and T. Potemra, 1989), and the assumption that the measured fluxes were at 90° pitch angles. Last, we converted to phase space density using the relation,

$$f(M, L) = 0.535(dJ/dE)A^2/E$$

where A is the atomic mass in amu, E is the energy in keV, dJ/dE is in particles/cm²-s-sr-keV, and f is in s³km⁻⁶.

Because the day-to-day variability in the magnetosphere is high, we constructed a second, geometrical average by taking logarithms of the flux before time averaging, and eliminating zero and negative fluxes. Simultaneously, we calculated the variance in the results from the individual orbital passes. Since discarding zeroes overestimates the low fluxes we did not use this aver-